Tissue non-linearity

F Duck
Medical Physics and Bioengineering Department, Royal United Hospital, Combe Park, Bath BA1 3NG, UK. email: f.duck@bath.ac.uk

The manuscript was received on 10 January 2009 and was accepted after revision for publication on 13 February 2009.

DOI: 10.1243/09544119JEIM574

Abstract: The propagation of acoustic waves is a fundamentally non-linear process, and only waves with infinitesimally small amplitudes may be described by linear expressions. In practice, all ultrasound propagation is associated with a progressive distortion in the acoustic waveform and the generation of frequency harmonics. At the frequencies and amplitudes used for medical diagnostic scanning, the waveform distortion can result in the formation of acoustic shocks, excess deposition of energy, and acoustic saturation. These effects occur most strongly when ultrasound propagates within liquids with comparatively low acoustic attenuation, such as water, amniotic fluid, or urine. Attenuation by soft tissues limits but does not extinguish these non-linear effects. Harmonics may be used to create tissue harmonic images. These offer improvements over conventional *B*-mode images in spatial resolution and, more significantly, in the suppression of acoustic clutter and side-lobe artefacts. The quantity B/A has promise as a parameter for tissue characterization, but methods for imaging B/A have shown only limited success. Standard methods for the prediction of tissue *in-situ* exposure from acoustic measurements in water, whether for regulatory purposes, for safety assessment, or for planning therapeutic regimes, may be in error because of unaccounted non-linear losses. Biological effects mechanisms are altered by finite-amplitude effects.

Keywords: acoustic non-linearity, finite-amplitude effects, biomedical ultrasound, tissue harmonic imaging, B/A

1 INTRODUCTION

The widespread introduction of harmonic imaging into ultrasound scanning during the past decade has served to emphasize the fundamental reality of the non-linear ultrasonics. While non-linear acoustic phenomena had been understood for well over a century [**1**, **2**], the early development of medical ultrasound largely ignored them. This view was based in part on the view that acoustic attenuation and scattering by soft tissues would serve to inhibit any of the known non-linear phenomena. It was only following the development of interest in non-linear acoustics for underwater applications that initial investigations in tissue non-linearity were considered. Since then there has been a growing awareness of non-linear ultrasound in the biomedical context, and several useful reviews have already been published [**3**–**5**]. It is the intention of the present short review to concentrate on the specific aspects of non-linearity relating to propagation through tissue, and only to deal briefly with those aspects of the fundamental acoustics necessary for immediate understanding. More extensive background material may be found elsewhere [**6**, **7**].

In 1980, two papers served to focus attention on the fact that finite-amplitude effects were important in biomedical ultrasound fields [**8**, **9**]. The term 'finite amplitude' is used to distinguish these beams from those described in basic acoustics texts where, for simplicity, a linear description of acoustic wave propagation is given. It is now understood that this approximation must be viewed with considerable caution, and that all ultrasound beams should be viewed as exhibiting some finite-amplitude characteristics unless shown otherwise. The effects are cumulative with path length, occur more readily at higher frequencies, and increase with increasing acoustic pressure and by focusing. These effects, described more fully below, include the distortion of the acoustic waveform, the associated generation of components at harmonic frequencies of the funda-

mental, and a local increase in acoustic attenuation resulting from harmonic generation and shock formation. Some or all of these effects occur in diagnostic pulses for imaging and Doppler, in physiotherapy beams, in high-intensity focused ultrasound (HIFU) beams for surgery, and beams for extra-corporeal lithotripsy. Only for continuous-wave beams for Doppler studies, e.g. for fetal heart monitoring, can the approximation of linear propagation be made with any confidence.

2 OUTLINE THEORY OF NON-LINEAR PROPAGATION

In this section those theoretical expressions essential to a basic understanding of finite-amplitude mechanisms will be presented. It is easiest first to consider an infinite plane wave travelling in a lossless medium. Figure 1 illustrates the progressive change in its acoustic pressure waveform. As an initially sinusoidal wave propagates, the peak compression progressively catches up with the zero crossing ahead of it, and the position of the peak rarefaction ahead of the zero crossing also becomes closer. Eventually all three positions coincide when the phase shift of the peak compression is $\pi/2$ and that of the peak rarefaction is $-\pi/2$. The pressure discontinuity so formed is called an acoustic shock; the peak compression follows immediately and discontinuously behind the peak decompression. As the wave propagates further, dissipation causes the acoustic shock progressively to diminish in magnitude, eventually attenuating to become a small-amplitude sinusoid.

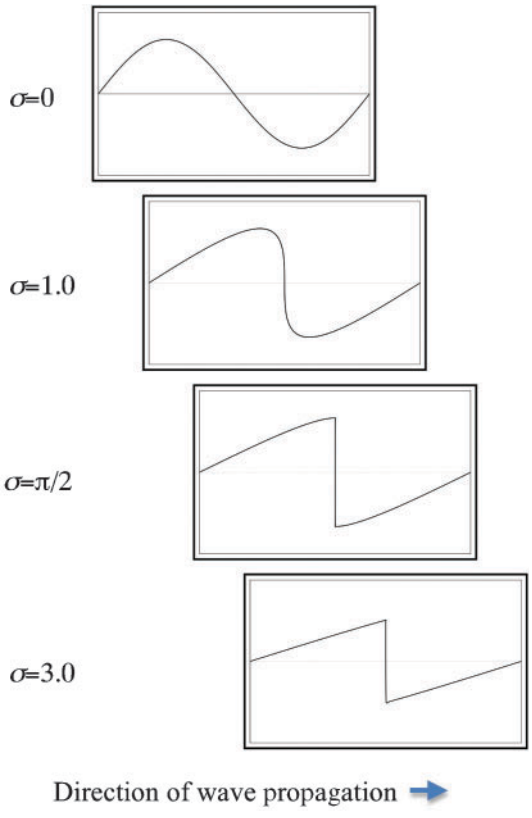

Fig. 1 The progressive change in acoustic pressure waveform with propagation for a single cycle of an infinite plane wave of finite amplitude. σ is defined in equation (2). The displacement of the images to the right is diagrammatic, indicating only that the cycle shown has moved forward as σ increases

The progressive change in shape arises from the variation in phase velocity v_θ at different points on the wave, being highest in the high-density compressions, and lowest in the low-density rarefactions. In fluids, a good approximation for the relationship between v_θ and the particle velocity u_θ can be derived from the non-linear wave equation

$$v_\theta = c_0 + \left(1 + \frac{B}{2A}\right) u_\theta \tag{1}$$

where c_0 is the wave velocity (i.e. the speed of travel of the zero crossings). The ratio B/A is a quantity that is proportional to the ratio of the coefficients of the quadratic and linear terms in the Taylor series expansion relating variations in pressure in a medium to variations in density (see any of the review material cited above). The quantity in parentheses, namely $1+B/2A$, is referred to as the coefficient of non-linearity β, of the medium. The phase velocity is thus equal to the wave velocity, modulated by a contribution depending on the particle velocity, itself made up of two parts. The first of these parts is convective, adding the particle velocity to the wave velocity. The second depends on B/A and is a property of the medium. For water and most soft tissues, about one third of the distortion arises from the convective component and two thirds from the properties of the medium.

The tendency for the waveform progressively to steepen as it propagates, causing discontinuities or shocks, leads to the concept of the shock formation distance or discontinuity length l_d. This is the distance at which an acoustic shock first forms, and l_d is given by

$$l_d = \frac{1}{\varepsilon \kappa \beta} \tag{2}$$

where ε, the acoustic Mach number, is u_0/c_0, where

u_0 is the peak particle velocity at the source, and κ is the wave number. At any other distance z, the distortion of the wave can be conveniently described using the shock parameter σ, where $\sigma = z/l_d$. From equation (2),

$$\sigma = \varepsilon\kappa\beta z \tag{3}$$

an equation which encapsulates with great simplicity the linear dependences of waveform shape on amplitude, frequency, material properties, and propagation distance.

The shock parameter is often used to refer to distorted waveforms in a part-quantitative part-descriptive way. For very low values of σ less than 0.1, the wave may justifiably be considered to be linear. $\sigma = 1$ is the threshold at which a pressure discontinuity has just formed at the zero crossing. $\sigma = \pi/2$ marks the formation of a full shock, and $\sigma = 3$ the formation of a sawtooth wave. While σ itself has no upper bound, the sawtooth wave at $\sigma = 3$ represents the greatest possible waveform distortion and harmonic generation in an infinite plane wave.

One outcome of the changed waveform illustrated in Fig. 1 is an alteration in the spectrum of the wave. A monochromatic wave progressively becomes richer in harmonic frequencies of the fundamental. For values of σ considerably less than 1.0, the magnitude of the second harmonic increases with the square of the acoustic pressure in the fundamental. The third and higher harmonics increase similarly, according to the power of the harmonic number n. As σ increases, the amplitude of the fundamental decreases because energy moves to the harmonic frequencies. At $\sigma = 1$, the second, third, and fourth harmonic amplitudes are 0.4 dB, 0.25 dB, and 0.18 dB respectively relative to the fundamental. With the formation of a sawtooth waveform at $\sigma = 3$ the harmonic amplitudes depend on $1/n$, and so the second, third, and fourth harmonics are 0.5 dB, 0.33 dB, and 0.25 dB respectively relative to the fundamental.

As the wave progressively distorts, the attenuation of the wave increases. This is caused by the absorption of the generated harmonics, an excess loss of energy arising from the frequency dependence of attenuation [**10**, **11**]. Under these conditions, the local attenuation coefficient may be described empirically as the sum of the attenuation components from the medium and from the shock. The contribution from the shock increases from a negligible value to close to its maximum value in the range $1 < \sigma < 3$. Once a shock has fully formed, the local attenuation becomes effectively independent of the medium [**12**]. However, as discussed below, the attenuation of the medium serves to inhibit the creation of an acoustic shock, and conditions under which attenuation is likely to become independent of the properties of the medium lie outside current conditions of biomedical ultrasound use. The excess attenuation associated with shock propagation ultimately leads to a further phenomenon, acoustic saturation. This describes the condition at any field point when any increase in source amplitude fails to cause an associated increase in field amplitude. Conditions approaching acoustic saturation can occur when pulses from ultrasonic scanners propagate in water [**4**].

3 NON-LINEAR PROPAGATION IN REAL ULTRASONIC BEAMS

The waves associated with medical applications of ultrasound differ in a number of important ways from the infinite plane wave described above, and these differences will now be reviewed. First, the amplitude of a real beam has strong spatial variations caused by diffraction. These affect the waveform distortion as the wave propagates. Figure 2 demonstrates the partial decomposition of a representative finite-amplitude beam in the near field, showing three of its frequency components. Their amplitude and phase summation, together with other harmonics not shown, give rise to large localized differences in waveform. Near-field minima fill with harmonics, as do the lobe boundaries throughout the field. Harmonic proportions do not follow simple trends, as would occur in an infinite plane wave, harmonic values approaching or even exceeding the local value of the fundamental. Phase variations between the fundamental frequency and its harmonics result in asymmetry in the distorted wave, often resulting in waves whose peak compression exceeds the magnitude of the peak rarefaction (Fig. 3). The shape and drive characteristics of array transducers, sometimes using astigmatism of focusing, may also cause unforeseen beam behaviour at large amplitudes, especially associated with exposure measurements in water [**13**]. For example, the position of the focal maximum may alter significantly and suddenly as the source amplitude alters [**14**, **15**], and harmonic peaks can be generated at the limits of diagonals [**16**, **17**].

Ultrasound diagnostic applications generally use short wide-bandwidth pulses. Distortion develops

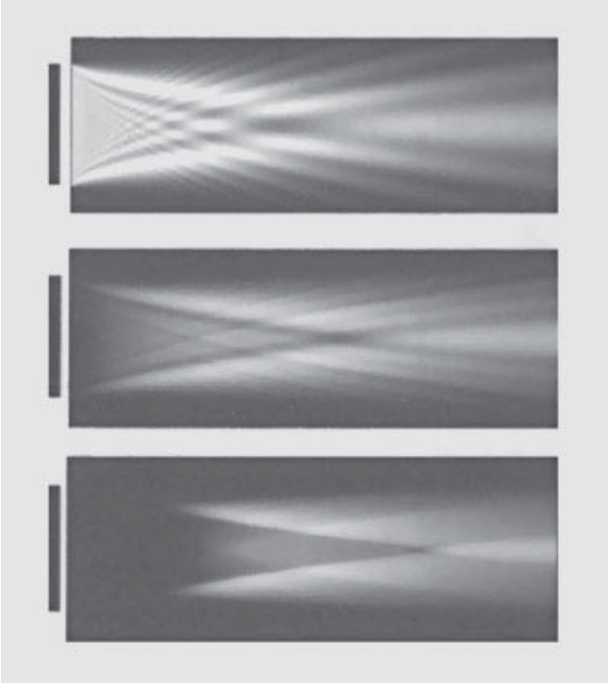

Fig. 2 Harmonic beam patterns in water predicted for a 2.25 MHz unfocused square source of side 20 mm and $p_0 = 1$ MPa. The beam patterns along a beam diagonal are shown, to a maximum distance of 200 mm. Shown from top to bottom, the fundamental, second-harmonic, and tenth-harmonic components. (Redrawn from Fig. 2.7 of reference [**18**])

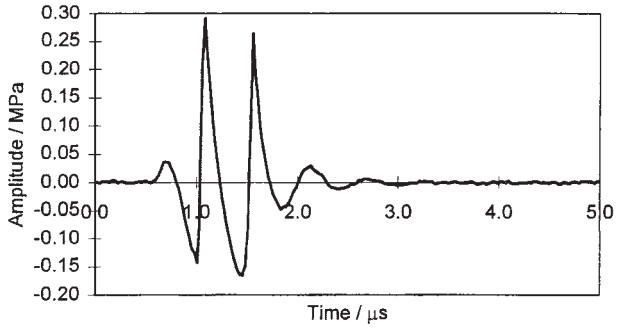

Fig. 3 Measured waveform of a 2.25 MHz imaging pulse in water at 600 mm showing typical non-linear distortion and asymmetry. Note that the distortion is largely restricted to the large-amplitude cycles in the middle of the pulse, leaving the small-amplitude cycles at the ends of the pulse largely unaffected

initially in the large-amplitude cycles of the pulse and, as the pulse propagates further, progressively extends to the smaller-amplitude cycles. The pulse spectrum develops maxima that are centred approximately on multiples of the centre frequency of the fundamental pulse spectrum (Fig. 4). Beam focusing gives local emphasis to finite-amplitude effects in the focal zone, both for weakly-focused diagnostic beams and more strongly focused beams such as those used in HIFU. In the pre-focal region the wave can alter from being unshocked to fully shocked over axial distances of a few millimetres. A practical non-linear parameter σ_m, has been developed to describe shock conditions at the focus, using an analysis of Gaussian beams of circular symmetry operating at a single frequency [**18**].

Finite-amplitude propagation is usually predicted using numerical computational approaches, and these have been reviewed in the general reviews cited above. A widely used approach is a finite-difference solution to an approximate non-linear wave equation known as the Khokhlov–Zablotskaya–Kuznetsov (KZK) equation [**19**]. In addition to non-linearity, this formulation also accounts for absorption and diffraction, giving it immediate relevance for modelling in a biomedical ultrasound context, because it can take account of beam geometry (source shape and focusing) and attenuation effects. One criticism of the KZK equation arises from the so-called parabolic, or paraxial, assumption made in its development. This means that the acoustic energy is assumed to propagate in a fairly narrow beam, an assumption that ceases to be valid as the source dimension approaches one wavelength, or when it is strongly focused. An alternative approach operates in the frequency domain using a spatial Fourier transform to calculate diffraction effects, and thus should have no restrictions on the position of the field points [**20**]. This has been particularly successful in predicting the fields generated by extracorporeal lithotriptors [**21**]. Several groups have published relevant modelling studies [**22**–**26**].

4 NON-LINEAR PROPAGATION IN SOFT TISSUES

The propagation of ultrasound through tissues is characterized by the same non-linear processes described above, modified by higher acoustic absorption. The tendency for wave distortion to occur is limited by attenuation of the fundamental and its harmonics. The balance between the non-linear processes, characterized by the coefficient of non-linearity β, and the dissipative (absorption) processes, characterized by the small-signal attenuation coefficient α at the fundamental frequency, is given by the Gol'dberg [**27**, **28**] number Γ, according to

$$\Gamma = \frac{\beta\varepsilon\kappa}{\alpha} = \frac{2\pi f p_0}{\rho_0 c_0^3}\frac{\beta}{\alpha} \tag{4}$$

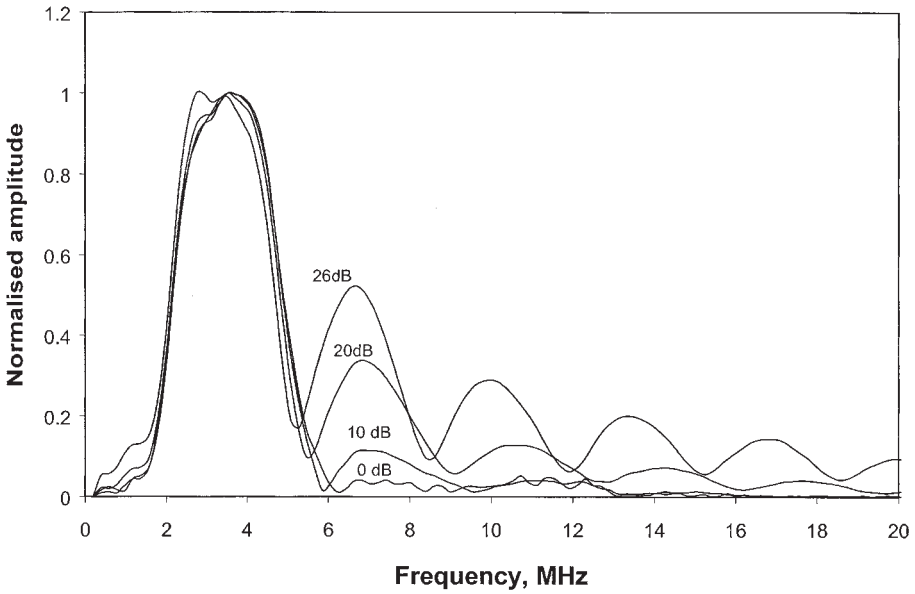

Fig. 4 Focal pulse spectra measured in water at 3.5 MHz, with a source of 19 mm diameter focused at 90 mm. The harmonic bands develop as the source amplitude is increased by 10 dB, 20 dB, and 26 dB from a near-linear condition

where p_0 is the acoustic pressure at the source. Γ may be considered as being the ratio l_a/l_d between two characteristic distances, where l_a is the absorption length and l_d is the discontinuity length (equation (2)). When $\Gamma \gg 1$, i.e. when the absorption length considerably exceeds the discontinuity length, non-linear processes dominate, as they do for diagnostic pulses in water. At diagnostic frequencies, the Gol'dberg number for soft tissue is about two orders of magnitude smaller than that for water, and so non-linear effects are much less evident. Haran and Cook [**29**] predicted waveform distortion under physiotherapy conditions and showed that attenuation in liver prevented the wave from becoming significantly distorted, because the Gol'dberg number never exceeded unity for the conditions investigated. Diagnostic beams are focused and use higher source pressures and frequencies than those used for therapy. Under these conditions, more strongly shocked conditions can be created in tissue (Fig. 5) [**30**, **31**]. There is some evidence that tissue scatter due to acoustic inhomogeneities has little effect on non-linear propagation [**32**].

A second consideration, when comparing propagation in water with that in tissue, is the non-linearity of the medium itself, as characterized by B/A. Table 1 gives some values and ranges of B/A for tissues and fluids [**33**]. B/A increases slowly with increasing temperature. For body fluids such as blood and urine, B/A is only slightly higher than water, and in soft tissues it increases with fat content to a maximum about twice that of water. This range is very small in comparison with the range of α, and thus it is attenuation that dominates the difference in non-linear behaviour between low-loss fluids and soft tissues. The preferred method of measurement is the thermodynamic method [**35–37**], replacing the less accurate finite-amplitude method [**38**, **39**], at least when large volumes of material are available. The thermodynamic method requires the measurement of sound velocity as a function of hydrostatic pressure and temperature.

In summary, frequency dependent absorption is the dominant acoustic property that distinguishes non-linear acoustic behaviour in soft tissue from that in low-loss fluids, such as water and amniotic fluid. Nevertheless, differences in B/A may also modify the degree to which distortion and harmonic generation occur.

5 BIOMEDICAL APPLICATIONS OF TISSUE NON-LINEARITY

The developing understanding of tissue non-linearity has led to the commercial development of tissue harmonic imaging, for which finite-amplitude effects have been exploited for the first time in clinical practice. These recent developments were preceded by a body of other work, however, which sought to exploit non-linear effects in other ways.

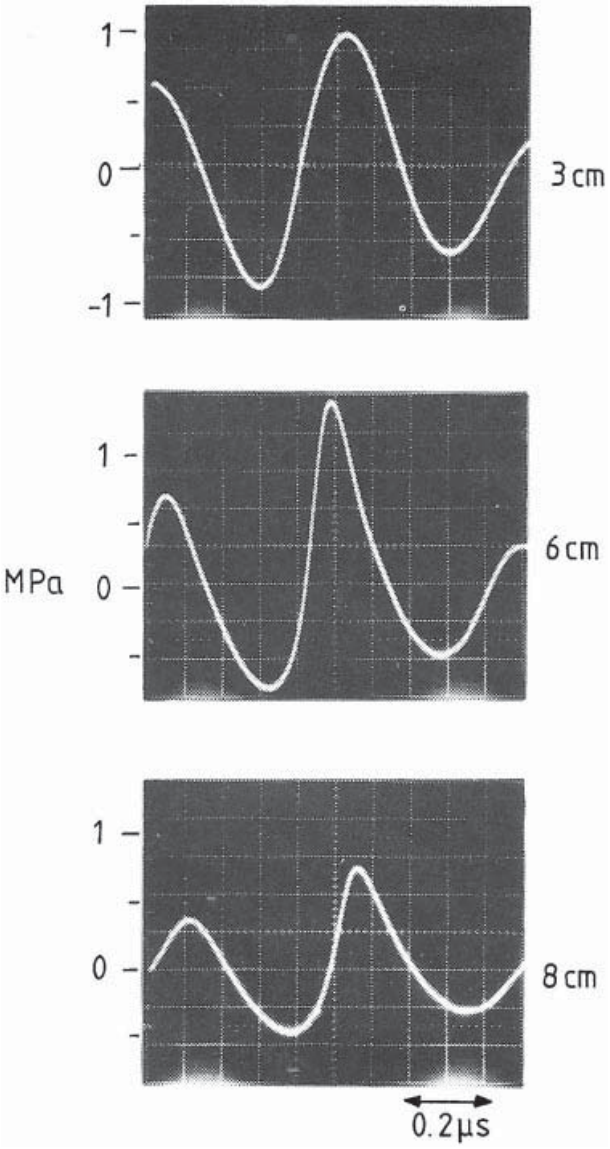

Fig. 5 Measured waveform distortion of a diagnostic pulse propagating through ox liver *in vitro* with a 2.5 MHz weakly-focused transducer and p_0 = 0.58 MPa. (Redrawn from Fig. 2 of reference [**31**])

Table 1 Measured values of B/A for some fluids and biological media (see p. 36 of reference [**7**] and references [**33**] and [**34**])

Medium	Temperature (°C)	*B*/*A*
Water	20	4.96
Water	40	5.38
3.5% saline	20	5.25
Blood plasma	30	5.74
Whole blood	26	6.1
Non-fatty soft tissues		6.3–8.0
Fatty soft tissues		9.6–11.3

5.1 Tissue characterization using *B*/*A*

B/*A* offers a potentially powerful parameter for tissue characterization. Fatty soft tissues are more strongly non-linear than those without fat (Table 1) [**40**, **41**]. In addition, other dependences have been reported. In biomolecular solutions, *B*/*A* depends on solution concentration but not on solute molecular weight [**42**]. *B*/*A* is strongly influenced by the character of the solvent–solute interaction and may be sensitive to molecular structural features [**43**]. There is also evidence that *B*/*A* is dependent on the ratio of free to bound water [**44**, **45**]. Structural features have been investigated, and *B*/*A* may also depend on structural complexity [**46**], including cell–cell adhesive forces, cellular structure, and secondary and tertiary protein structure. *B*/*A* is reported to be independent of perfusion [**47**].

Given this evidence, the motivation to develop means to measure and image *B*/*A* *in vivo* are considerable. Most efforts have pursued transmission tomographic techniques. These include a system to image *B*/*A* using an impulsive high-power pumping wave (1 cycle of 500 kHz) applied perpendicular to a continuous low-intensity 5 MHz probing wave [**48**]. The phase of the probing wave is modulated by the instantaneous product of *B*/*A* and pumping acoustic pressure. Images of the human forearm with rather poor spatial resolution were demonstrated. An alternative approach used the second-harmonic amplitude as its basis [**49**, **50**]. Harmonic generation through the sample was compared with that through a reference medium. Images were obtained of porcine tissues *in vitro*.

Transmission imaging has failed to result in convincing results, however, and is difficult to apply in a clinical situation. Methods using a single transducer in pulse-echo mode offer more practical promise. One method used a high-frequency probe and pump waves propagating in opposite directions, generating a *B*/*A* profile along the propagation path in real time [**51**]. While such a method may be applied with the transducer on one side, by using an acoustic reflector, the method is still somewhat impractical. A similar criticism may be made of an alternative approach [**52**], by which bulk *B*/*A* is derived by detecting echoes at progressively increasing acoustic output and observing the deviation from linearity of the transducer input–output relationship. A realistic review of current progress has been published [**53**]. In summary, although the laboratory evidence has encouraged the exploration of *B*/*A* as a parameter for tissue characterization, imaging methods have so far been unable to exploit this potential.

5.2 Tissue harmonic imaging

Tissue harmonic imaging was created as an offshoot of the development of harmonic methods for gas-bubble contrast imaging. While contrast imaging is an interesting topic in its own right, space precludes its inclusion in this review.

Early studies in acoustic microscopy had suggested that improved resolution could be achieved using second and higher harmonics [**54**, **55**]. Parametric imaging, developed for underwater imaging [**56**, **57**], was explored for biomedical applications [**58**]. In this technique a carrier wave of high directionality (say, at 10 MHz) is modulated at a lower frequency such that a narrow beam of low-frequency sound is generated by non-linear mixing in the medium. Several early reports demonstrated the potential to improve lateral resolution through imaging second and higher harmonics in pulse-echo imaging [**59**–**62**], but it was always possible to argue that such improvements might be gained by simply using a higher fundamental frequency. The significant evidence, which followed the clinical use of harmonic imaging systems designed for use with contrast agents, was the improved signal-to-noise ratio resulting from the reduction in acoustic noise in harmonic images. These cleaner images were particularly noticeable when scanning patients who were known to be difficult to examine ultrasonically, e.g. because of obesity or poor acoustic windows. Furthermore, diagnostic artefacts such as shadowing and acoustic enhancement may be better defined [**63**].

A number of factors may contribute to the improvement in image clarity. All arise because the second harmonic depends on the square of the fundamental amplitude. Echoes with large second-harmonic amplitudes arise, therefore, most particularly from tissues on the beam axis, where the pulse amplitude not only is the greatest but also retains the largest amplitude throughout its path. Under a number of situations, the pulse amplitude is small for all or much of its path and, as a result, there is a relative reduction in the proportion of generated harmonic. For example, at the edges of the beam, the pulse amplitude is smaller than on the axis and harmonics are poorly generated. Echoes from off-axis objects of high reflectivity remain primarily in the fundamental band and do not appear in a second-harmonic image. Similarly, reverberant pulses travel largely at small amplitudes and the harmonic content will be limited to only that generated by the transmission to the target. Secondary and tertiary scattering events give rise to pulses of small amplitude, adding no additional harmonic during the scattering process. Image artefacts from multiple scattering will be therefore suppressed in harmonic imaging. Harmonic imaging also offers another means to manage grating lobes. Each of these factors contribute to a reduction in the acoustically generated noise in the image, and this in turn gives rise to images which can exploit the available electronic dynamic range more completely.

Several techniques have been developed to extract the harmonic signal. The most obvious is to apply a high-pass filter to the received signal [**64**]. This method is now uncommon, since depth resolution must be compromised in order to create a well-defined cut-off frequency between the fundamental and harmonic pulse spectra. The deficiencies of harmonic filtering have been largely overcome by the development of pulse (or phase) inversion [**65**–**67**]. Two sequential pulses are used, usually directed along exactly the same path. The second pulse is phase reversed, compressions becoming rarefactions and vice versa. The reflected signal following the first pulse is stored and added to that from the second pulse, cancelling the fundamental frequency f_0 and leaving only the even harmonics of the original wave. The process is demonstrated for a pulse in Fig. 6. The two main disadvantages of phase inversion arise from the need to use two pulses rather than only one. This not only halves the frame rate but also introduces the possibility of movement-generated artefact. The bandwidth of the transducer gives a practical limit to the range of harmonic frequencies that may be used, typically restricting it to include only the second harmonic. In order to exploit the wider range of harmonics, one experimental system describes the use of an array of very wide bandwidth, pulsed at a low fundamental frequency (1.2 MHz). The method, called 'superharmonic imaging' demonstrated increased signal-to-noise ratio, improved contrast, and acceptable penetration depth [**68**]. Linear FM chirp excitation has also been proposed as a means to improve the signal-to-noise ratio [**69**]. In clinical practice it has been found to be advantageous to combine the harmonic image with that created at either f_0 or $2f_0$. At least one commercial scanner uses dual-frequency pulses in pulse inversion mode, so combining the advantages of conventional and tissue harmonic imaging [**70**].

The clinical usefulness of harmonic imaging became rapidly established [**71**–**73**]. Examples of pairs of scans showing the improved image quality that may be achieved are shown in Fig. 7 (adult cardiac scan) and Fig. 8 (renal cyst). Reports have

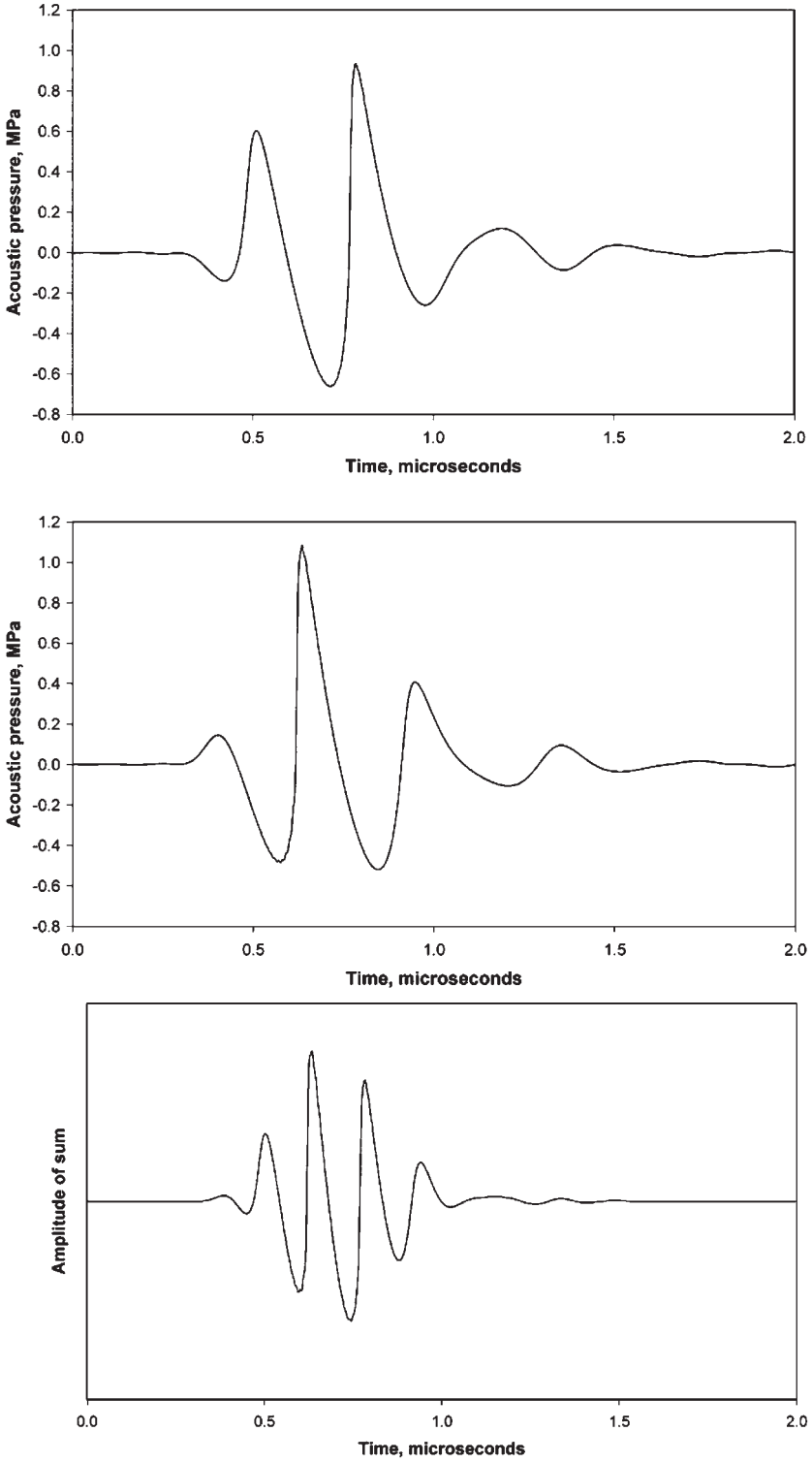

Fig. 6 Demonstration of the principle of pulse inversion harmonic imaging predicted using numerical calculation for typical diagnostic pulses ($p_0 = 0.5$ MPa; $f_0 = 3$ MHz; rectangular focused 1.0 cm × 1.5 cm source; pulses computed at 80 mm, at the focus in tissue with an attenuation coefficient of 0.3 dB/cm MHz; $\beta = 3.5$). The upper two waveforms are from pulses that differ only in being phase inverted from one another at the source. The bottom pulse shows the wave shape of their sum. (From Fig. 10 of reference [**4**]: computation by Dr Mark Cahill)

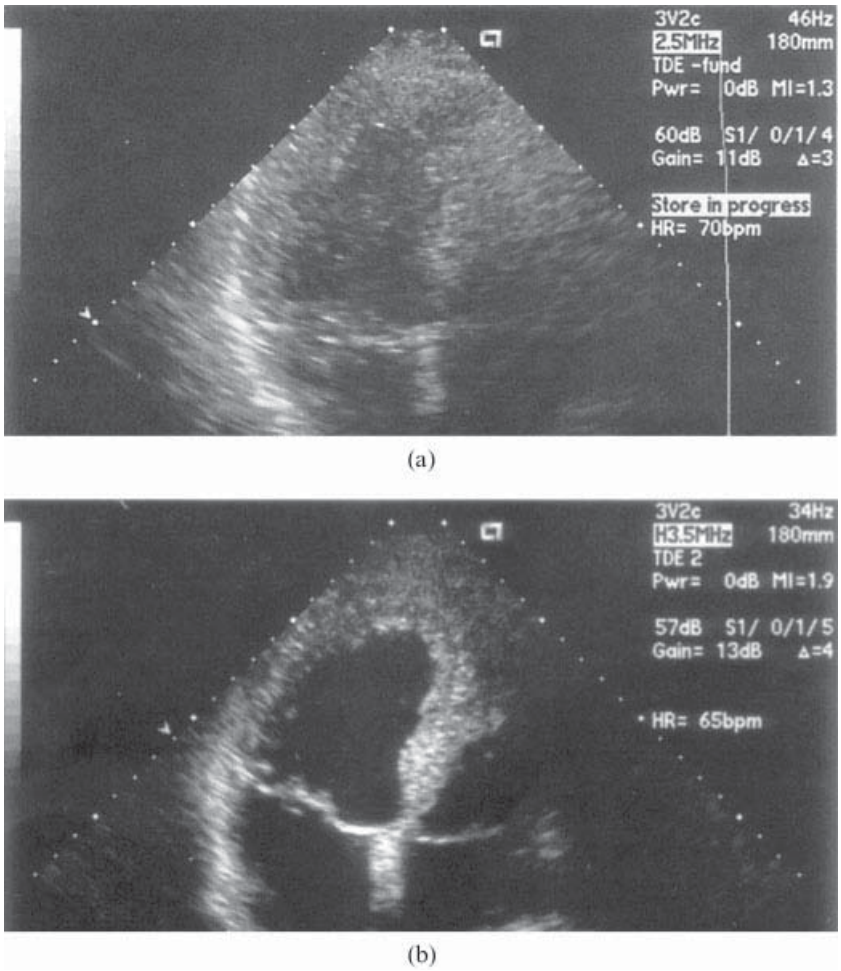

Fig. 7 Images showing the improvement achieved by using harmonic imaging for adult cardiac scanning: (a) conventional (fundamental) pulse-echo image with significant acoustic clutter filling the ventricular spaces in the image; (b) equivalent tissue harmonic image demonstrating reduced clutter, and improved resolution

demonstrated the diagnostic value of tissue harmonic imaging in obstetrics [**74**], in general abdominal and pelvic imaging [**75**], in hepatic [**76**], pancreatic [**77**], renal [**78**], and breast imaging [**79**, **80**], in cardiology [**81**, **82**] and in musculoskeletal studies [**83**]. The most obvious advantages arise when examining otherwise difficult-to-image patients. Particularly valuable is the ability to distinguish between clutter and structure within fluid spaces such as the gall bladder, the pregnant uterus, and suspected cysts. Edges of structures are better defined. These successes are encouraging the investigation of harmonic imaging with intravascular transducers at higher frequencies [**84**].

6 ESTIMATING *IN-SITU* EXPOSURE IN THE PRESENCE OF NON-LINEARITY

As was noted above, non-linear propagation changes and attenuates the acoustic wave. This is most noticeable during acoustic measurements in water, e.g. of acoustic pressure [**85**] and acoustic power [**86**] and of acoustically generated heating [**87**]. As a result, considerable care must be taken when using such measurements to estimate exposure within the body, for example when using such measurements to calculate safety indices [**88**]. There are now strong experimental and theoretical grounds to challenge the validity of present linear procedures for estimating *in-situ* exposure [**89**], for which the errors in estimating attenuated exposures by using linear attenuation correction may be over 50 per cent depending on the beam and position of measurement. At the highest levels, acoustic saturation can result in regulatory limits being ineffective, since they are based on linear estimates of *in-situ* exposure [**90**].

A number of methods have been proposed for the management of non-linear loss for *in-situ* exposure estimation. Water has significant advantages over any other liquid as the medium in which to make standard

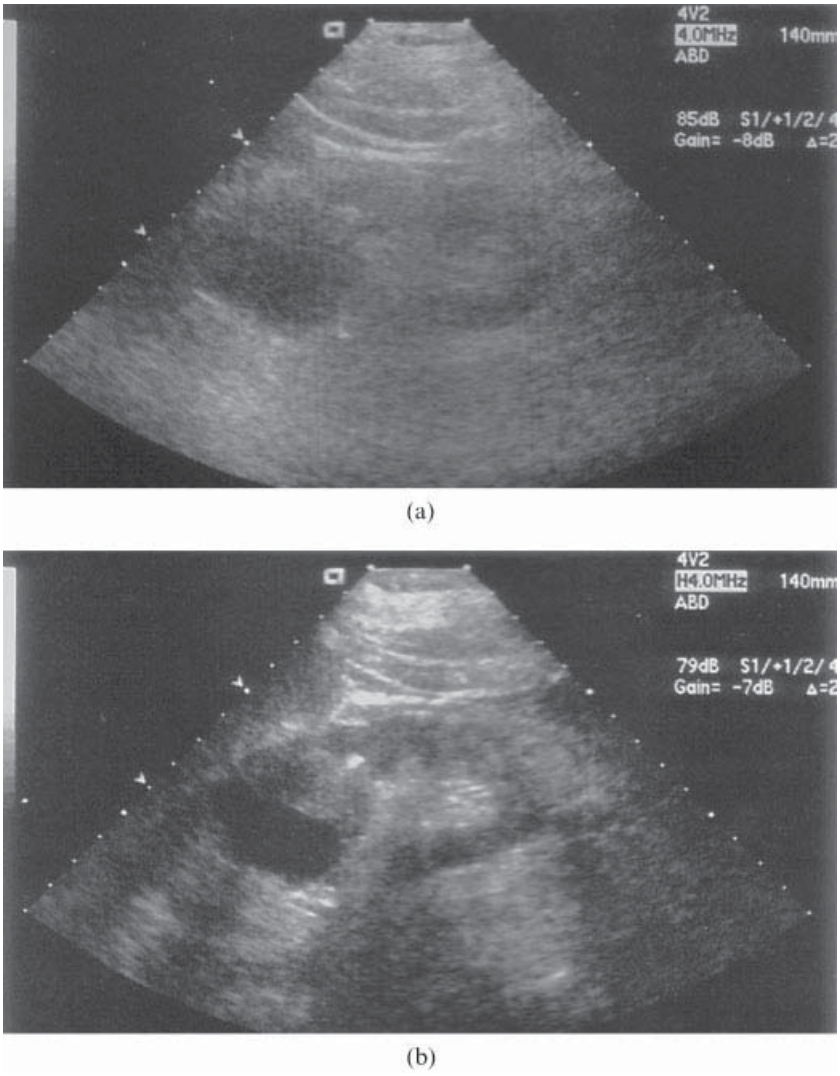

Fig. 8 Images showing the improvement achieved by harmonic imaging for a difficult-to-image renal cyst: (a) conventional (fundamental) pulse-echo image; (b) tissue harmonic image showing improved visualization of the cystic mass

acoustic measurements. As a result the International Electrotechnical Commission (IEC) [**91**] has proposed a standard method to ensure that all measurements are carried out in water under defined 'quasi-linear' conditions. In this IEC technical specification, these conditions are set by ensuring that the local distortion factor σ_q in water is less than 0.5, where

$$\sigma_q = z p_m \frac{2\pi f \beta}{\rho_0 c_0^3} \frac{1}{\sqrt{F_a}} \tag{5}$$

p_m is the average of the peak compressional and peak rarefactional pressures, and F_a is an expression for the beam area relative to that at the source (equivalent to the local amplitude gain). The rationale for the limiting value arises from considerations of non-linear energy dissipation in the transmission path [**92**]. Control of acoustic amplitude may be achieved either by electronic attenuation of the output drive level or acoustic attenuation using calibrated plastic attenuators [**93**, **94**]. Once the measurements are made, any appropriate model may be used to estimate *in-situ* exposure at higher levels, scaled appropriately from acoustic pressures measured close to the transducer.

Alternative approaches are available, nevertheless. For example, measurements may be made under known non-linear conditions, and the values corrected for the estimated excess loss of energy [**95**, **96**]. The beam must be numerically modelled to give a correction value [**97**, **98**]. Alternatively, water may be replaced by a liquid that has appropriate tissue-like acoustic properties. The liquid could have an attenuation coefficient of 0.3 dB/cm MHz, and both

speed of sound and B/A should be appropriate [**99**]. Other tissue-equivalent liquids may have acoustic attenuation coefficients closer to those of soft tissues and biological fluids [**34**]. Early compositions of tissue-mimicking liquids resulted in values of B/A of about 5.7, rather below that of most fat-free soft tissues [**100**]. However, a more recent study of nine alternative formulations reported that B/A in the non-fat mimics ranged from 5.6 to 6.6 and for fatty tissue mimics from 9.8 to 11.1 [**101**]. By selecting an appropriate liquid mimic, it has been possible to study the errors associated with the linear assumptions that underpin current methods for estimating *in-situ* exposure [**102**]. Large errors can arise when calculating the safety indices used by operators to ensure patient safety [**103**], and this experimental study confirmed earlier predictions made on the basis of exposure measurements in water [**104–106**]. There are therefore now several methods with which it is possible to avoid the institutionalized errors in estimating *in-situ* exposure. Such methods will, in the future, improve the regulatory process underpinning the safety of diagnostic ultrasound exposure, by ensuring that the displayed safety indices have greater scientific validity. Furthermore, as concepts of acoustic dose develop [**107**], dose planning for surgery and therapy will require techniques such as these to ensure that appropriate exposure regimes are prescribed.

7 ALTERED BIOLOGICAL EFFECTS MECHANISMS DUE TO TISSUE NON-LINEARITY

Non-linearity alters biological effects mechanisms. Enhancement of heating from the absorption of harmonics in the beam has implications for hyperthermia [**108**] and in diagnostic applications [**109**]. Early studies suggested that temperature rises could be enhanced by a factor of up to 3, the numerical enhancement correlating well with the value of the shock parameter. Under conditions of non-linear propagation, the maximum heating migrates towards the pre-focal region in a homogeneous tissue [**110**]. For safety considerations, attention has been given to enhancement beyond a low-loss fluid path, such as might exist during obstetric scanning. Modelling and experimental measurement using layered models relevant to obstetric scanning suggest that temperature increases up to 50 per cent greater than in the linear case may be reached, although, at larger amplitudes, heating can be inhibited owing to non-linear dissipation in the fluid path [**111–113**].

Acoustic shock significantly enhances the velocity of acoustic streaming generated by diagnostic pulses [**114**], and numerical methods have been developed to predict these effects [**115**]. This mechanism probably accounts in part for the streaming observed during clinical studies [**116**], suggesting that it may be common for pulses to become strongly shocked in fluid spaces *in vivo*. A study by Zauhar *et al.* [**117**] found no difference between the streaming velocity generated in water and amniotic fluid by large-amplitude pulses while, in a low-amplitude continuous-wave field, faster streaming was caused in amniotic fluid. For the large-amplitude pulses, non-linear effects dominated while, at low amplitudes, the different absorption coefficients between the fluids caused the difference in streaming velocities. The associated enhancement in radiation force has also been calculated [**118**], predicting an approximately fourfold increase in soft tissue when comparing a sawtooth wave with a sinusoidal wave.

8 SUMMARY

The propagation of acoustic waves is a non-linear process. For many situations in medical ultrasound, linear assumptions fail. For example, a backscattered second harmonic can be detected and imaged, a process for which linear acoustic analysis gives no explanation. Absorption of harmonics enhances temperature rise and acoustic streaming. Acoustic shocks may be generated and conditions approaching acoustic saturation may be achieved. Regulatory boundaries based on linear assumptions fail. There is an extensive theoretical understanding of the principles underlying non-linear effects. While the quantity B/A seems promising for tissue characterization, methods for imaging B/A have only shown limited success. Detailed predictions of non-linear effects require numerical methods needing substantial computing power and further development. Such modelling is required to understand and develop fully tissue harmonic imaging, now widely integrated into mainstream diagnostic ultrasound practice. Correct prediction of exposure and energy deposition for therapeutic, surgical, and safety purposes also requires a clear understanding of non-linear propagation. Standard methods are now available to avoid the institutionalized errors in estimating *in-situ* exposure, and such methods should enhance the integrity of exposure and dose estimation.

REFERENCES

1 **Stokes, G. G.** On a difficulty on the theory of sound. *Phil. Mag., Ser. 3*, 1848, **33**, 349–356.
2 **Airy, G. B.** On a difficulty in the problem of sound. *Phil. Mag., Ser. 3*, 1849, **34**, 401–405.
3 **Carstensen, E. L.** and **Bacon, D. R.** Biomedical applications. In *Nonlinear acoustics* (Eds M. F. Hamilton and D. T. Blackstock), 1998, ch. 15, pp. 421–447 (Academic Press, San Diego, California).
4 **Duck, F. A.** Nonlinear acoustics in diagnostic ultrasound. *Ultrasound Medicine Biology*, 2002, **28**, 1–18.
5 **Szabo, T. L.** Nonlinear acoustics and imaging. *Diagnostic ultrasound imaging inside out*, 2004, ch. 12, pp. 381–427 (Elsevier Academic Press, San Diego, California).
6 **Beyer, R. T.** *Nonlinear acoustics*, 1997 (Acoustical Society of America, Melville, New York (reprint of original published by the Naval Ship Systems Command, Washington, DC, 1974)).
7 **Hamilton, M. F.** and **Blackstock, D. T.** *Nonlinear acoustics*, 1998 (Academic Press, San Diego, California).
8 **Carstensen, E. L., Law, W. K., McKay, N. D.,** and **Muir, T. G.** Demonstration of nonlinear acoustical effects at biomedical frequencies and intensities. *Ultrasound Medicine Biology*, 1980, **6**, 359–368.
9 **Muir, T. G.** and **Carstensen, E. L.** Prediction of nonlinear acoustic effects at biomedical frequencies and intensities. *Ultrasound Medicine Biology*, 1980, **6**, 345–357.
10 **Baker, A. C.** A numerical study of the effect of drive level on the intensity loss from an ultrasonic beam. *Ultrasound Medicine Biology*, 1997, **23**, 1083–1088.
11 **Dalecki, D., Carstensen, E. L.,** and **Parker, K. J.** Absorption of finite amplitude focused ultrasound. *J. Acoust. Soc. Am.*, 1991, **89**, 2435–2447.
12 **Carstensen, E. L., McKay, N. D., Dalecki, D.,** and **Muir, T. G.** Absorption of finite amplitude ultrasound in tissues. *Acustica*, 1982, **1**, 116–123.
13 **Cahill, M. D.** and **Baker, A. C.** Numerical simulation of the acoustic field of a phased-array medical ultrasound scanner. *J. Acoust. Soc. Am.*, 1998, **104**, 1274–1283.
14 **Duck, F. A.** Estimating *in situ* exposure in the presence of acoustic nonlinearity. *J. Ultrasound Medicine*, 1999, **18**, 43–53.
15 **Cahill, M. D.** and **Humphrey, V. F.** The effect of nonlinear propagation on measurements of mechanical index. *Ultrasound Medicine Biology*, 2000, **26**, 433–440.
16 **Cahill, M. D.** and **Baker, A. C.** Increased off-axis energy deposition due to diffraction and nonlinear propagation from rectangular sources. *J. Acoust. Soc. Am.*, 1997, **102**, 119–203.
17 **Baker, A. C.** Nonlinear effects in ultrasonic propagation. In *Ultrasound in Medicine* (Eds F. A. Duck, A. C. Baker, and H. C. Starritt), 1998, pp. 23–38 (IoP Publishing, Bristol).
18 **Bacon, D. R.** Finite amplitude distortion of the pulsed fields used in diagnostic ultrasound. *Ultrasound Medicine Biology*, 1984, **10**, 189–195.
19 **Kuznetsov, V. P.** Equations of nonlinear acoustics. *Soviet Physics Acoust*, 1971, **16**, 467–470.
20 **Christopher, T.** and **Parker, K. J.** New approaches to nonlinear diffractive field propagation. *J. Acoust. Soc. Am.*, 1991, **90**, 488–499.
21 **Christopher, T.** Modeling the Dornier HM3 lithotripter. *J. Acoust. Soc. Am.*, 1994, **95**, 3088–3095.
22 **Lee, Y.-S.** and **Hamilton, M. F.** Time-domain modeling of pulsed finite-amplitude sound beams. *J. Acoust. Soc. Am.*, 1995, **97**, 906–917.
23 **Li, Y.** and **Zagzebski, J. A.** Computer model for harmonic ultrasound imaging. *IEEE Trans. Ultrasonics Ferroelectrics Frequency Control*, 2000, **47**, 1259–1272.
24 **Baker, A. C., Berg, A. M., Sahin, A.,** and **Naze Tjøtta, J.** The nonlinear pressure field of plane, rectangular apertures: experimental and theoretical results. *J. Acoust. Soc. Am.*, 1995, **97**, 3510–3517.
25 **Zemp, R. J., Tavakkoli, J.,** and **Cobbold, R. S. C.** Modeling of nonlinear ultrasound propagation in tissue from array transducers. *J. Acoust. Soc. Am.*, 2003, **113**, 139–152.
26 **Yang, X.** and **Cleveland, R. O.** Time domain simulation of nonlinear acoustic beams generated by rectangular pistons with application to harmonic imaging. *J. Acoust. Soc. Am.*, 2005, **117**, 113–123.
27 **Gol'dberg, Z. A.** Second approximation acoustic equations and the propagation of plane waves of finite amplitude. *Soviet Physics Acoust.*, 1956, **2**, 346–350.
28 **Gol'dberg, Z. A.** On the propagation of plane waves of finite amplitude. *Soviet Physics Acoust.*, 1957, **3**, 340–347.
29 **Haran, M. E.** and **Cook, B. D.** Distortion of finite amplitude ultrasound in lossy media. *J. Acoust. Soc. Am.*, 1983, **73**, 774–779.
30 **Starritt, H. C., Perkins, M. A., Duck, F. A.,** and **Humphrey, V. F.** Evidence for ultrasonic finite-amplitude distortion in muscle using medical equipment. *J. Acoust. Soc. Am.*, 1985, **77**, 302–306.
31 **Starritt, H. C., Duck, F. A., Hawkins, A. J.,** and **Humphrey, V. F.** The development of harmonic distortion in pulsed finite-amplitude ultrasound passing through liver. *Physics Medicine Biology*, 1986, **31**, 1401–1409.
32 **Christopher, T.** Finite amplitude distortion-based inhomogeneous pulse echo ultrasonic imaging. *IEEE Trans. Ultrasonics Ferroelectrics Frequency Control*, 1997, **44**, 125–139.
33 **Duck, F. A.** *Physical properties of tissue: a comprehensive reference book*, 1990, p. 98 (Academic Press, London).
34 International Commission on Radiation Units and Measurements, Tissue substitutes, phantoms and

computational modelling in medical ultrasound. ICRU Report 61, 1998 (Bethesda, Maryland, USA).
35 **Coppens, A. B., Beyer, R. T., Seiden, M. B., Donohue, J., Guepin, F., Hodson, R. H.,** and **Townsend, C.** Parameter of nonlinearity in fluids. II. *J. Acoust. Soc. Am.*, 1965, **38**, 797–804.
36 **Sehgal, C. M., Bahn, R. C.,** and **Greenleaf, J. F.** Measurement of the acoustic nonlinearity parameter B/A in human tissues by a thermodynamic method. *J. Acoust. Soc. Am.*, 1984, **76**, 1023–1029.
37 **Zhang, J.** and **Dunn, F.** A small volume thermodynamic system for B/A measurement. *J. Acoust. Soc. Am.*, 1991, **89**, 73–79.
38 **Beyer, R. T.** Parameter of nonlinearity in fluids. *J. Acoust. Soc. Am.*, 1960, **32**, 719–721.
39 **Law, W. K., Frizzell, L.,** and **Dunn, F.** Determination of the nonlinearity parameter B/A of biological media. *Ultrasound Medicine Biology*, 1985, **11**, 307–318.
40 **Errabolu, R. L., Sehgal, C. M., Bahn, R. C.,** and **Greenleaf, J. F.** Measurement of ultrasonic nonlinear parameter in excised fat tissues. *Ultrasound Medicine Biology*, 1988, **14**, 137–146.
41 **Sehgal, C. M., Brown, G. M., Bahn, R. C.,** and **Greenleaf, J. F.** Measurement and use of acoustic nonlinearity and sound speed to estimate composition of excised livers. *Ultrasound Medicine Biology*, 1986, **12**, 865–874.
42 **Law, W. K., Frizzell, L.,** and **Dunn, F.** Ultrasonic determination of the nonlinearity parameter B/A for biological media. *J. Acoust. Soc. Am.*, 1981, **69**, 1210–1212.
43 **Sarvazyan, A. P., Chalikian, T. V.,** and **Dunn, F.** Acoustic nonlinearity parameter B/A of aqueous solutions of some amino acids and proteins. *J. Acoust. Soc. Am.*, 1990, **88**, 1555–1561.
44 **Sehgal, C. M.** and **Greenleaf, J. F.** Correlative study of properties of water in biological systems by using ultrasound and magnetic resonance. *Magn. Resonance Medicine*, 1986, **3**, 976–985.
45 **Yoshizumi, K., Sato, T.,** and **Ichida, N.** A physicochemical evaluation of the nonlinear parameter B/A for media predominantly composed of water. *J. Acoust. Soc. Am.*, 1987, **82**, 302–305.
46 **Zhang, J., Kuhlenschmidt, M. S.,** and **Dunn, F. R.** Influences of structural factors of biological media on the acoustic nonlinearity parameter B/A. *J. Acoust. Soc. Am.*, 1991, **89**, 80–91.
47 **Zhang, J.** and **Dunn, F.** *In vivo* B/A determination in a mammalian organ. *J. Acoust. Soc. Am.*, 1987, **81**, 1635–1637.
48 **Ichida, N., Takuso, S., Miwa, H.,** and **Murakami, K.** Real-time nonlinear parameter tomography using impulsive pumping waves. *IEEE Trans. Sonics Ultrasonics*, 1984, **31**, 635–641.
49 **Zhang, D., Gong, X. F.,** and **Ye, S. G.** Acoustic nonlinearity parameter tomography for biological specimens via measurement of the second harmonics. *J. Acoust. Soc. Am.*, 1996, **99**, 2397–2402.
50 **Zhang, D.** and **Gong, X.** Experimental investigation of acoustic nonlinearity parameter tomography for excised pathological biological tissues. *Ultrasound Medicine Biology*, 1999, **25**, 593–599.
51 **Cain, C. A.** Ultrasonic reflection mode imaging of the nonlinear parameter B/A: I. Theoretical basis. *J. Acoust. Soc. Am.*, 1986, **80**, 28–32.
52 **Nikoonahad, M.** and **Liu, D. C.** Pulse-echo single frequency acoustic nonlinearity parameter (B/A) measurement. *IEEE Trans. Ultrasonics Ferroelectrics Frequency Control*, 1990, **37**, 127–134.
53 **Zhang, D.** and **Gong, X.** Acoustic nonlinear imaging and its application in tissue characterization. In Proceedings of the Fourth International Workshop on *Ultrasonic and advanced methods for nondestructive testing and material characterization*, University of Massachusetts, Dartmouth, Massachusetts, USA, 19 June 2006, available from http://www.ndt.net/article/vllh07/papers/01.php3.
54 **Kompfner, R.** and **Lemons, R. A.** Nonlinear acoustic microscopy. *Appl. Physics Lett.*, 1976, **28**, 295–297.
55 **Germain, L.** and **Cheeke, J. D. N.** Generation and detection of high-order harmonics in liquids using a scanning acoustic microscope. *J. Acoust. Soc. Am.*, 1988, **83**, 942–949.
56 **Berktay, H. O.** Parametric amplification by the use of acoustic nonlinearities and some possible applications. *J. Sound Vibr.*, 1965, **2**, 462–470.
57 **Westervelt, P. J.** Parametric acoustic array. *J. Acoust. Soc. Am.*, 1963, **35**, 535–537.
58 **Bjørnø, L.** and **Grinderslev, S.** Parametric echoscanner for medical diagnosis. *J. Physique, Coll, C8*, 1979, **40**, C8-111–C8-118.
59 **Muir, T. G.** Nonlinear effects in acoustic imaging. *Acoust. Imaging*, 1980, **9**, 93–109.
60 **Bjørnø, L.** and **Lewin, P. A.** Nonlinear focusing effects in ultrasonic imaging. In Proceedings of the IEEE Ultrasonics Symposium, 1982, pp. 659–662 (IEEE, New York).
61 **Ward, B., Baker, A. C.,** and **Humphrey, V. F.** Nonlinear propagation applied to the improvement of resolution in diagnostic medical ultrasound equipment. *J. Acoust. Soc. Am.*, 1997, **101**, 143–154.
62 **Humphrey, V. F.** Nonlinear propagation in ultrasonic fields: measurements, modelling and harmonic imaging. *Ultrasonics*, 2000, **38**, 267–272.
63 **Desser, T. S., Jesrzejewicz, T.,** and **Bradley, C.** Native tissue harmonic imaging: basic principles and clinical applications. *Ultrasound Q.*, 2000, **16**, 40–48.
64 **Averkiou, M. A., Roundhill, D. N.,** and **Powers, J. E.** A new imaging technique based on the nonlinear properties of tissues. In Proceedings of the IEEE Ultrasonics Symposium, 1997, pp. 1561–1566 (IEEE, New York).
65 **Chapman, C. S.** and **Lazenby, J. C.** Ultrasound imaging system employing phase inversion subtraction to enhance the image. US Pat. 5,632,277, 1997.

66 **Wright, N. J., Maslak, S. H., Finger, D. J.,** and **Gee, A.** A method and apparatus for coherent image formation. US Pat. 5,667,373, 1997.

67 **Jang, H. J., Lim, H. K., Lee, W. J., Kim, S. H., Kim, K. A.,** and **Kim, E. Y.** Ultrasonographic evaluation of focal hepatic lesions: comparison of pulse inversion harmonic, tissue harmonic, and conventional imaging techniques. *J. Ultrasound Medicine*, 2000, **19**, 293–299.

68 **Bouakaz, A.** and **de Jong, N.** Native tissue harmonic imaging at superharmonic frequencies. *IEEE Trans. Ultrasonics Ferroelectrics Frequency Control*, 2003, **50**, 469–506.

69 **Arshadi, R., Yu, A. C. H.,** and **Cobbold, R. S. C.** Coded excitation methods for ultrasound harmonic imaging. *Can. Acoust.*, 2007, **35**, 35–46.

70 **Chiou, S-Y., Fosberg, F., Fox, T. B.,** and **Needleman, L.** Comparing differential tissue harmonic imaging with tissue harmonic and fundamental gray scale imaging of the liver. *J. Ultrasound Medicine*, 2007, **26**, 1557–1563.

71 **Haerten, R., Lowery, C., Becker, G., Gebel, H., Rosenthal, S.,** and **Sauerbrei, E.** Ensemble™ tissue harmonic imaging: the technology and clinical utility. *Electromedica*, 1999, **97**, 50–56.

72 **Tranquart, F., Grenier, N., Eder, V.,** and **Pourcelot, L.** Clinical use of ultrasound tissue harmonic imaging. *Ultrasound Medicine Biology*, 1999, **25**, 889–894.

73 **Rosenthal, S. J., Jones, P. H.,** and **Wetzel, L. H.** Phase inversion tissue harmonic sonographic imaging: a clinical utility study. *Am. J. Roetgenology*, 2001, **176**, 1393–1398.

74 **Ryu, J., Kim, B., Kim, S., Yang, S. H., Choi, M. H.,** and **Ahn, H. S.** Ultrasound evaluation of normal and abnormal fetuses: comparison of conventional, tissue harmonic, and pulse-inversion imaging techniques. *Korean J. Radiology*, 2003, **4**, 184–190.

75 **Desser, T. S., Jeffrey, R. B., Lane, M. J.,** and **Ralls, P. W.** Pictorial essay: utility of tissue harmonic imaging in abdominal and pelvic ultrasonography. *J. Clin. Ultrasound*, 1999, **27**, 135–141.

76 **Tanaka, S., Oshikawa, O., Saski, T.,** and **Tsukama, H.** Evaluation of tissue harmonic imaging for the diagnosis of focal hepatic lesions. *Ultrasound Medicine Biology*, 2000, **26**, 183–187.

77 **Hohl, C., Schmidt, T., Haage, P., Honnef, D., Blaum, M., Staatz, G.,** and **Guenther, R. W.** Phase-inversion tissue harmonic imaging compared with conventional *B*-mode ultrasound in the evaluation of pancreatic lesions. *Eur. Radiology*, 2004, **14**, 1109–1117.

78 **Schmidt, T., Hohl, C., Haage, P., Blaum, M., Honnef, D., Weiss, C., Staatz, G.,** and **Günther, R. W.** Diagnostic accuracy of phase-inversion tissue harmonic imaging versus fundamental *B*-mode sonography in the evaluation of focal lesions of the kidney. *Am. J. Roentgenology*, 2003, **180**, 1639–1647.

79 **Szopinski, K. T., Pajik, A. M., Wysocki, M., Dominique, A., Szopinska, M.,** and **Jakubowski, W.** Tissue harmonic imaging; utility in breast sonography. *J. Ultrasound Medicine*, 2003, **22**, 479–487.

80 **Mesurolle, B., Helou, T., El-Khoury, M., Edwardes, M., Sutton, E. J.,** and **Kao, E.** Tissue harmonic imaging, frequency compound imaging, and conventional imaging: use and benefit in breast sonography. *J. Ultrasound Medicine*, 2007, **26**, 1041–1051.

81 **Kornbluth, M., Liang, D. H., Paloma, A.,** and **Schnittger, I.** Native harmonic imaging improves endocardial border definition and visualisation of cardiac structures. *J. Am. Soc. Echocardiography*, 1998, **11**, 693–701.

82 **Shapiro, R. S., Wagreich, J., Parsons, R. B., Stancato-Pasik, A., Yeh, H. C.,** and **Lao, R.** Tissue harmonic imaging sonography: evaluation of image quality compared with conventional sonography. *Am. J. Roentgenology*, 1998, **171**, 1203–1206.

83 **Strobel, K., Zanetti, M., Nagy, L.,** and **Hodler, J.** Suspected rotator cuff lesions: tissue harmonic imaging versus conventional US of the shoulder. *Radiology*, 2004, **230**, 243–249.

84 **Frijlink, M. E., Goertz, D. E., van Damme, L. C. A., Krams, R.,** and **van der Steen, A. F. W.** Intravascular ultrasound tissue harmonic imaging *in vivo*. In Proceedings of the IEEE Ultrasonics Symposium, 2004, vol. 2, pp. 1118–1121 (IEEE, New York).

85 **Duck, F. A.** and **Starritt, H. C.** The spatial distribution of excess absorption in water due to shock transmission. *Physics Medicine Biology*, 1989, **34**, 1623–1631.

86 **Duck, F. A.** and **Perkins, M. A.** Amplitude-dependent losses in ultrasound exposure measurement. *IEEE Trans. Ultrasonics Ferroelectrics Frequency Control*, 1988, **35**, 232–241.

87 **Duck, F. A.** and **Starritt, H. C.** A study of the heating capabilities of diagnostic ultrasound beams. *Ultrasound Medicine Biology*, 1994, **20**, 481–492.

88 IEC 62359 *Ultrasonics – field characterization – test methods for the determination of thermal and mechanical indices related to medical diagnostic ultrasound fields*, 2006 (International Electrotechnical Commission, Geneva).

89 **Christopher, T.** and **Carstensen, E. L.** Finite amplitude distortion and its relationship to linear derating formulae for diagnostic ultrasound systems. *Ultrasound Medicine Biology*, 1996, **22**, 1103–1116.

90 **Duck, F. A.** Acoustic saturation and output regulation. *Ultrasound Medicine Biology*, 1999, **25**, 1009–1018.

91 IEC 61949 *Ultrasonics – field characterization – in-situ exposure estimation in finite-amplitude ultrasonic beams*, 2007 (International Electrotechnical Commission, Geneva).

92 **Duncan, T., Humphrey, V. F.,** and **Duck, F. A.** A numerical comparison of nonlinear indicators for diagnostic ultrasound fields. In Proceedings of the Fifth World Congress on Ultrasonics, Paris, France, 7–10 September 2003, pp. 85–88, CD-ROM.

93 **Preston, R. C., Shaw, A.,** and **Zeqiri, B.** Prediction of *in situ* exposure to ultrasound: an acoustical attenuation method. *Ultrasound Medicine Biology*, 1991, **17**, 317–332.

94 **Preston, R. C., Shaw, A.,** and **Zeqiri, B.** Prediction of *in situ* exposure to ultrasound: a proposed standard experimental method. *Ultrasound Medicine Biology*, 1991, **17**, 333–339.

95 **Bacon, D. R.** Prediction of *in situ* exposure to ultrasound: an improved method. *Ultrasound Medicine Biology*, 1989, **15**, 355–361.

96 **Verma, P. K., Humphrey, V. F.,** and **Starritt, H. C.** Enhanced absorption due to nonlinear propagation in diagnostic ultrasound. In Advances in nonlinear acoustics, Proceedings of the 13th International Symposium on *Nonlinear acoustics* (Ed. H. Hobæk). Bergen, Norway, 1993, pp. 297–302 (World Scientific, Singapore).

97 **Bacon, D. R.** and **Baker, A. C.** Comparison of two theoretical models for predicting nonlinear propagation in medical ultrasound fields. *Physics Medicine Biology*, 1989, **34**, 1633–1643.

98 **Baker, A. C.** A numerical study of the effect of drive level on the intensity loss from an ultrasonic beam. *Ultrasound Medicine Biology*, 1997, **23**, 1083–1088.

99 **Jiang, P., Everbach, E. C.,** and **Apfel, R. E.** Application of mixture laws for predicting the composition of tissue phantoms. *Ultrasound Medicine Biology*, 1991, **17**, 829–838.

100 **Macdonald, M. C.** and **Madsen, E. L.** Acoustic measurements in a tissue mimicking liquid. *J. Ultrasound Medicine*, 1999, **18**, 55–62.

101 **Dong, F., Madsen, E. L., MacDonald, M. C.,** and **Zagzebski, J. A.** Nonlinearity parameter for tissue-mimicking materials. *Ultrasound Medicine Biology*, 1999, **25**, 831–838.

102 **Stiles, T. A., Madsen, E. L., Frank, G. R., Diehl, T.,** and **Lucey, J. A.** Tissue-mimicking liquid for use in exposimetry. *J. Ultrasound Medicine*, 2005, **24**, 501–516.

103 **Stiles, T. A.** *Diagnostic ultrasound exposimetry using a tissue-mimicking liquid*. PhD Dissertation, University of Wisconsin-Madison, Wisconsin, USA, 2005.

104 **Szabo, T. L., Clougherty, F.,** and **Crossman, C.** Effects of nonlinearity on the estimation of *in situ* values of acoustic output parameters. *J. Ultrasound Medicine*, 1999, **18**, 33–41.

105 **Carstensen, E. L., Dalecki, D., Gracewski, S. M.,** and **Christopher, T.** Nonlinear propagation and the output indices. *J. Ultrasound Medicine*, 1999, **18**, 69–80.

106 **Christopher, T.** Computing the mechanical index. *J. Ultrasound Medicine*, 1999, **18**, 63–68.

107 **Duck, F. A.** Acoustic dose and acoustic dose rate. *Ultrasound in Medicine Biology*, 2009 (in press).

108 **Swindell, W.** A theoretical study of nonlinear effects with focused ultrasound in tissues: an 'acoustic Bragg peak'. *Ultrasound Medicine Biology*, 1985, **11**, 121–130.

109 **Bacon, D. R.** and **Carstensen, E. L.** Increased heating by diagnostic ultrasound due to nonlinear propagation. *J. Acoust. Soc. Am.*, 1990, **88**, 26–34.

110 **Meaney, P. M., Cahill, M. D.,** and **ter Haar, G. R.** The intensity dependence of lesion position shift during focused ultrasound surgery. *Ultrasound Medicine Biology*, 2000, **26**, 441–450.

111 **Wójcik, J., Filipczyński, L.,** and **Kujawska, T.** Temperature elevations computed for three-layer and four-layer tissue models in nonlinear and linear ultrasonic propagation cases. *Ultrasound Medicine Biology*, 1999, **25**, 259–267.

112 **Divall, S. A.** and **Humphrey, V. F.** Finite difference modelling of the temperature rise in nonlinear medical ultrasound fields. *Ultrasonics*, 2000, **38**, 273–277.

113 **Cahill, M. D., Humphrey, V. F., Doody, C.,** and **Duck, F. A.** The effect of nonlinear propagation on heating of tissue: numerical modelling and experimental measurement. In Proceedings of the IEEE Ultrasonics Symposium, 2002, pp. 1395–1398 (IEEE, New York).

114 **Starritt, H. C., Duck, F. A.,** and **Humphrey, V. F.** An experimental investigation of streaming in pulsed diagnostic ultrasound beams. *Ultrasound Medicine Biology*, 1989, **15**, 363–373.

115 **Kamakura, T., Matsuda, K., Kumamoto, Y.,** and **Breazeale, M. A.** Acoustic streaming induced in focused Gaussian beams. *J. Acoust. Soc. Am.*, 1995, **97**, 2740–2746.

116 **Duck, F. A.** Acoustic streaming and radiation pressure in diagnostic applications: what are the implications? In progress in obstetrics and gynaecology series (Eds S. B. Barnett and G. Kossoff), *Safety of diagnostic ultrasound*, 1998, pp. 87–98 (Parthenon, New York).

117 **Zauhar, G., Duck, F. A.,** and **Starritt, H. C.** Comparison of the acoustic streaming in amniotic fluid and water in medical ultrasonic beams. *Ultraschall Medizin (Eur. J. Ultrasound)*, 2006, **27**, 152–158.

118 **Starritt, H. C., Duck, F. A.,** and **Humphrey, V. F.** Forces acting in the direction of propagation in pulsed ultrasound fields. *Physics Medicine Biology*, 1991, **36**, 1465–1474.

APPENDIX

Notation

B/A	quantity derived from Taylor coefficients for the non-linearity of a medium

c_0	wave velocity	z	distance in the direction of wave propagation
f	ultrasonic frequency		
f_0	fundamental ultrasonic frequency		
F_a	local area factor	α	small-signal attenuation coefficient
l_d	discontinuity length; shock formation distance	β	coefficient of non-linearity = $1 + B/2A$
		Γ	Gol'dberg number = l_a/l_d
l_a	absorption length	ε	Mach number = u_0/c_0
n	harmonic number	κ	wave number = $2\pi/\lambda$
p_m	average of peak compression and peak rarefaction	λ	wavelength
		ρ_0	ambient density
p_0	peak acoustic pressure at source	σ	shock parameter
u_θ	particle velocity	σ_m	non-linear parameter (applicable at the focus)
u_0	peak particle velocity at source		
v_θ	phase velocity	σ_q	local distortion factor